Grass Research

ARTICLE

Open Access

https://doi.org/10.48130/grares-0026-0031

Grass Research **2026**, 6: e034

Characterization of *ZIP* genes that are involved in Cd resistance and accumulation in *Amaranthus hypochondriacus*

Xinyue Cao[1], Hanyang Wu[1], Wangchen Yu[1], Minhao Pan[1], Xiaobao Luo[1], Chuancheng Wang[1], Ningfang Liu[1], Qian Xu[1,2], Longxing Hu[1,2,3*] and Rui Lu[1,2*]

[1] *College of Agronomy, Hunan Agricultural University, Changsha 410128, China*
[2] *Yuelushan Laboratory, Changsha 410128, China*
[3] *Academician Workstation of Agricultural High-Tech Industrial Area of the Yellow River Delta, National Technology Innovation Center for Saline-Alkali Agriculture, Dongying 257300, China*
* Correspondence: grass@hunau.edu.cn (Hu L); ruilu@hunau.edu.cn (Lu R)

Abstract

The molecular mechanisms underlying cadmium (Cd) hyperaccumulation in plants remain largely unclear, particularly regarding the functional roles of the *zinc–iron permease* (*ZIP*) family genes in *Amaranthus hypochondriacus* L., a well-known Cd hyperaccumulator. In this study, the Cd hyperaccumulator *A. hypochondriacus* was used to identify *ZIP* family genes at the whole-genome level and to investigate their expression and function under cadmium stress. Analysis of the gene structures and conserved motifs revealed functional differentiation among subfamilies. Expression analysis showed that *AhZIP* genes exhibited tissue-specific expression patterns, and their expression levels were affected by Cd treatment. Heterologous expression of *AhZIP3/5/6* significantly enhanced Cd accumulation and sensitivity in Cd-sensitive yeast mutants (*ycf1*), indicating its role in promoting Cd uptake. This study preliminarily reveals the function of *AhZIP* genes in Cd accumulation and tolerance, providing a theoretical basis and genetic resources for improving phytoremediation efficiency through genetic engineering.

Keywords: *A. hypochondriacus*, ZIP, Cadmium stress, Cadmium hyperaccumulation, Heavy metal transporter

Citation: Cao X, Wu H, Yu W, Pan M, Luo X, et al. 2026. Characterization of *ZIP* genes that are involved in Cd resistance and accumulation in *Amaranthus hypochondriacus*. *Grass Research* 6: e034 https://doi.org/10.48130/grares-0026-0031

Introduction

With the development of agriculture and industries in recent years, heavy metal contamination in agricultural soils has become a non-negligible problem threatening agricultural production, food safety, human health, and environmental safety[1]. A nationwide research in China revealed that 19.4% of the investigated agricultural soils are suffering heavy metal pollution, and cadmium (Cd) contamination ranks first among the heavy metals (7%)[2]. Cd is a highly toxic and mobile metal element that can easily accumulate in plants and get into the food chain, threatening public health[3]. Therefore, it is urgent to remedy heavy metal-contaminated soil to reduce the risk to human health. Phytoremediation is a popular remediation method to manage heavy metal-contaminated soil and refers to using Cd-(hyper)accumulating plants to take up Cd from soil and thereby reduce the content of Cd in the soils[4,5]. Compared with traditional chemical and physical remediation methods, phytoremediation is cost-effective as well as eco-friendly and considered as a more promising method to repair the Cd-contaminated soil[6].

Several plants have been identified as Cd hyperaccumulators for the remediation of Cd-contaminated soils[7]. Among these accumulators, *Amaranthus hypochondriacus* is considered to be a more efficient Cd hyperaccumulator because of its merits of rapid growth, high biomass, easy cultivation, strong adaptability, and Cd hyperaccumulation[8]. In many studies, *A. hypochondriacus* has been extensively used to remedy Cd-contaminated agricultural soils[9,10], but the molecular mechanism of cadmium super enrichment in *A. hypochondriacus* is still unknown.

Understanding the regulatory mechanism for uptake, transport, and accumulation of Cd is critical for developing strategies of hyperaccumulation. There are no specific transporters for Cd, and plant roots usually take up toxic Cd ions into cells via transporters for essential metal ions, such as Mn^{2+}, Fe^{2+}, Cu^{2+}, and Zn^{2+}[11,12]. Several types of transporters in model plants and some hyperaccumulators have been found to function in the absorption and transport of Cd^{2+}[13]. For example, the members of the zinc–iron permease (ZIP) family, the natural resistance associated macrophage protein (NRAMP) family, and the heavy metal adenosine triphosphatase (HMA) family play significant roles in Cd^{2+} accumulation in plants[14,15].

Since ZIP family proteins are important transporters for the uptake and transport of essential metals, such as Zn, Fe, Mn, and Cu, many studies have been conducted to identify their functions in different varieties of plants[16]. The functions of ZIP family members for metal transport in *Arabidopsis thaliana* and rice (*Oryza sativa* L.) have been functionally characterized in the past few years.

In *A. thaliana*, AtIRT1's role as an iron-regulated metal transporter was first identified by its functional expression in yeast[17]. AtIRT1 was further found to play roles in the uptake of Zn, Mn, Co, Ni, and Cd from the rhizosphere to root cells[18]. It is also reported that the specific expression of AtIRT1 in phloem companion cells reveals its role in iron translocation in aboveground plant organs[19]. AtIRT2 localizes in the vesicle membrane and cooperates with the high-affinity iron uptake system to maintain iron homeostasis in roots' epidermal cells[20]. AtIRT3 functions as a plasma membrane-localized Zn and Fe uptake transporter[21]. AtZIP1 is a vacuolar transporter and is involved in remobilizing Mn and Zn from the vacuole to the cytoplasm in roots' stelar cells. AtZIP2 localizes in the plasma

© The Author(s)

https://doi.org/10.48130/grares-0026-0031

membrane, mediates Mn and Zn uptake into xylem parenchyma, and is responsible for subsequent xylem loading and transport to the shoot[22]. AtZIP3 is involved in the absorption of Zn from the soil to the plant roots, whereas AtZIP4 mediates the transportation of Zn intracellularly or between plant tissues[23].

In rice, two Fe transporters, OsIRT1 and OsIRT2, play roles in directly absorbing Fe^{2+} and Zn^{2+} into root cells[24]. OsZIP1 functions as a metal efflux transporter to avoid excess Zn, Cu, and Cd accumulation in rice[25]. OsZIP4 is suggested to be involved in the distribution of Zn within plants[26]. OsZIP5 and OsZIP8 function in Zn uptake and translocation within rice[27,28]. OsZIP7 plays a key role in xylem loading in roots and intervascular transfer in nodes to deliver Zn/Cd to developing tissues and grain[29]. OsZIP5 and OsZIP9 function synergistically in Zn/Cd uptake in rice roots[30].

ZIP family members have been reported in *Fagopyrum tataricum* L. Gaertn.[31], *Brassica rapa* L. ssp. *chinensis*[32], rice[33], *Brassica juncea* L.[34], *Triticum turgidum* ssp. *dicoccoides*[35], *Nicotiana tabacum* L.[36], and *Arachis hypogaea* L.[37]. However, there is still little information regarding ZIPs in *A. hypochondriacus* plants. The whole genome sequences with high-quality assembly of *A. hypochondriacus* has been released[38]. These studies laid the foundation for identifying *ZIP* genes at the whole-genome level. In our present study, the *ZIP* genes were identified genome-wide and detailed characteristics of the ZIP sequences were described. The expression patterns of *AhZIP* genes under Cd stress in roots and leaves were analyzed, and the function of AhZIP members in Cd uptake was confirmed by a Cd tolerance assay in yeast. Our findings will be valuable for further functional investigation and phytoremediation application of members of this gene family in *A. hypochondriacus*.

Materials and methods

Plant materials

A. hypochondriacus germplasm 'E94196' (PI 677035) was used in this study. The seeds were germinated in a seedling tray containing substrate sand and nutrient soil. The seedlings with a third true leaf were transferred to a hydroponic device containing a half-strength Hoagland nutrient solution. After 10 d of hydroponic culture, the Cd^{2+} stress treatment was conducted by supplementing a solution of 80 μM $CdCl_2$. Roots and leaves were harvested after 0, 1, 6, and 24 h of $CdCl_2$ treatment, frozen immediately in liquid nitrogen, and stored at –80 °C until RNA extraction.

Identification of *AhZIP* genes

To identify *ZIP* genes in *A. hypochondriacus*, all published *ZIP* gene sequences of *A. thaliana* and *O. sativa* were used as queries to perform homologous BLAST searches against the *A. hypochondriacus* genome databases (https://phytozome-next.jgi.doe.gov/info/Ahypochondriacus_v2_1)[38]. Furthermore, the conserved domains of predicted ZIP proteins were evaluated using the Hmmscan program and the Pfam tools (www.ebi.ac.uk/Tools/hmmer/search/hmmscan) according to reported methods[39].

Phylogenetic analysis

Multiple sequence alignments were conducted on the identified ZIP protein sequences in *A. hypochondriacus*, *A. thaliana*, and rice genomes by the MUSCLE alignment method using MEGA12 software. Given the results of multiple sequence alignment, MEGA12 software was used to construct an unrooted phylogenetic tree based on alignments using the neighbor-joining (NJ) method with the following parameters: Number of differences model, pairwise deletion, and 1,000 bootstraps[40]. Then the unrooted phylogenetic tree was subjected to Interactive Tree Of Life (iTOL) (http://itol.embl.de/upload.cgi) to form the interactive tree.

Analysis of chromosomal distribution and duplication of genes

The physical locations of *AhZIP* genes on the chromosomes were obtained by searching against the *A. hypochondriacus* genome databases (https://phytozome-next.jgi.doe.gov/report/gene/Ahypochondriacus_v2_1). All the *AhZIP* genes were mapped on the chromosomes using CorelDRAW X7 software.

Conserved motifs and transmembrane domain analysis

To identify the conserved protein motifs, the ZIP protein sequences were submitted to the online Multiple Expectation maximization for Motif Elicitation (MEME) (http://meme-suite.org/tools/meme) program. The optimized MEME parameters are as follows: Any number of repetitions, optimum width from 6 to 100, and the number of motifs to search for was 15.

Gene structure analysis

The gene sequences and coding sequences (CDSs) of *AhZIP* were identified from the *A. hypochondriacus* genome databases described above. The gene structure display server program (http://gsds.cbi.pku.edu.cn) was used to infer the exon–intron organization of *ZIP* genes.

Analysis of gene expression based on transcriptome data

To clarify the tissue-specific expression patterns of *AhZIP* genes in *A. hypochondriacus*, the reads per kilobase of transcript per million mapped reads (RPKM) values of each *AhZIP* gene, which represent the gene expression levels, were retrieved from the species-specific transcriptome database of *A. hypochondriacus* (BioProject ID: PRJNA290113, www.ncbi.nlm.nih.gov/bioproject/290113).

RNA isolation and real-time polymerase chain reaction analysis

Total RNA was extracted from the collected materials using a Tiangen RNAprep Pure Plant Kit according to the manufacturer's instructions. In total, 2 μg RNA was used as the template for the synthesis of first-strand cDNA using M-MLV reverse transcriptase (Vazyme, Nanjing, China) according to the manufacturer's instructions. Gene expression levels were analyzed by real-time polymerase chain reaction (RT-PCR) using the fluorescent intercalating dye SYBR Green in a detection system (ABI, QuantStudio 1, USA). The expression values of the tested *ZIP* genes were normalized, with the *AhActin* (*β-actin*) gene from *A. hypochondriacus* serving as the internal reference[41]. The relative expression levels (R) were calculated using the following equation: $R = 2^{-(Ct1 - Ct2)}$, where Ct1 refers to the Ct value of *AhZIP* genes and Ct2 is the Ct value of the reference gene. The RT-PCR data are mean values and standard deviations (shown as bars) of three independent experiments with three biological replicates. Based on the values of the relative expression levels, heatmaps for gene expression patterns were generated by the online program Omicshare (www.omicshare.com/tools/Home/Soft/heatmap). All primers used are listed in Supplementary Table S1.

Construction of the vectors and yeast tolerance assays

The coding sequences of *AhZIP* were cloned into the expression vector *pYES2* under the control of the GAL1 promoter. The recombinant vectors *pYES2-AhZIPs* were transferred into the *ycf1* mutant yeast strain (*Saccharomyces cerevisiae*) and then the positive yeast transformants were tested on Synthetic Dextrose Minimal Medium lacking Uracil (SD/Ura) medium. For drop tests, the yeast suspension was serially diluted to an optical density at 600 nm (OD_{600}) of 0.2, 0.02, and 0.002; 5 μL of each serial dilution was dropped onto SD/Ura medium (containing 2% galactose and 1% raffinose) with different concentrations of $CdCl_2$. For measuring the growth curve, the yeast transformants were incubated in Synthetic Complete dropout medium lacking Uracil (SC/Ura) medium (containing 2% galactose and 1% raffinose) with 40 μM $CdCl_2$ incubated for 48 h, during which the OD values were measured every 8 h.

Analysis of Cd contents

Cells of each line (1×10^7) were added to 30 mL of SD-Ura liquid medium containing 60 μM $CdCl_2$ and then cultured for 48 h at 30 °C. The cells were then collected and washed twice with distilled water and digested with HNO_3 and H_2O_2 (3:1) at 140 °C for 10 min, 200 °C for 20 min, and 140 °C for 10 min. All of samples were analyzed to detect total Cd by using inductively coupled plasma optical emission spectrometry (ICP-OES; ThermoFisher ICAP 6300, Waltham, MA, USA). All analyses were repeated three times.

Statistical analysis

All experiments were performed with three independent biological replicates, and the data are expressed as the mean ± standard deviation (SD). Statistical analyses were performed using Origin 2021 and Microsoft Excel 2021. For comparisons among multiple groups, one-way analysis of variance (ANOVA) followed by Tukey's honestly significant difference (HSD) *post hoc* test was used. A *p*-value < 0.05 was considered to be statistically significant, and different lowercase letters above the bars in the figures indicate significant differences between groups. For comparisons between two groups, Student's *t*-test (two-tailed, unpaired) was used, and significance levels were indicated as * $p < 0.05$, ** $p < 0.01$, and *** $p < 0.001$.

Results

Characterization and chromosomal distribution of the *AhZIP* gene family

To identify all *ZIP* genes in *A. hypochondriacus* genome, a BLASTP search against the *A. hypochondriacus* genome database was performed by using all published *ZIP* sequences of *A. thaliana* and rice as queries. Finally, after the removal of repeats and a search of the conserved ZIP domain by the Hmmscan online website, 14 *ZIP* genes were identified in *A. hypochondriacus*[39]. They were designated as *AhZIP1–14* according to their chromosomal locations to give them uniform names. The amino acid number of newly verified AhZIP proteins varied from 275 to 596, harboring 5–16 transmembrane (TM) domains (Supplementary Table S2 and Supplementary Fig. S1). The molecular weight of AhZIP proteins ranged from 29.46 to 62.02 kDa, and the theoretical isoelectric points (pI) of AhZIP proteins ranged from 5.83 to 8.83 (Supplementary Table S2).

The physical locations of *AhZIP* genes suggested that *AhZIP* genes are unevenly distributed across 6 of the 16 *A. hypochondriacus* chromosomes (Fig. 1). Chr1 contained four *AhZIP* genes, Chr11 contained three, Chr2 contained one, and Chr6, Chr9, and Chr15 each contained two *AhZIP* genes.

Phylogenetic analysis of AhZIP proteins

To elucidate the phylogenetic relationships and evolutionary characteristics of the AhZIP protein family in *A. hypochondriacus*, phylogenetic trees were constructed in this study using 14 AhZIP proteins from *A. hypochondriacus*, 14 AtZIP proteins from *A. thaliana*, and 12 OsZIP proteins from rice (Fig. 2). The results showed that all ZIP family members could be clearly divided into three major clades (Clade I, Clade II, and Clade III). Among them, Clade I was the smallest clade, containing only one member, AhZIP14, with no OsZIP proteins detected; Clade II was the second largest clade, consisting of all 12 OsZIP proteins, with no AtZIP or AhZIP proteins detected; and Clade III was the largest clade, comprising 27 members, including 13 AhZIP proteins and 14 AtZIP proteins, without OsZIP proteins detected. ZIP proteins from different species exhibited obvious species-specific distribution patterns across the three clades: OsZIP

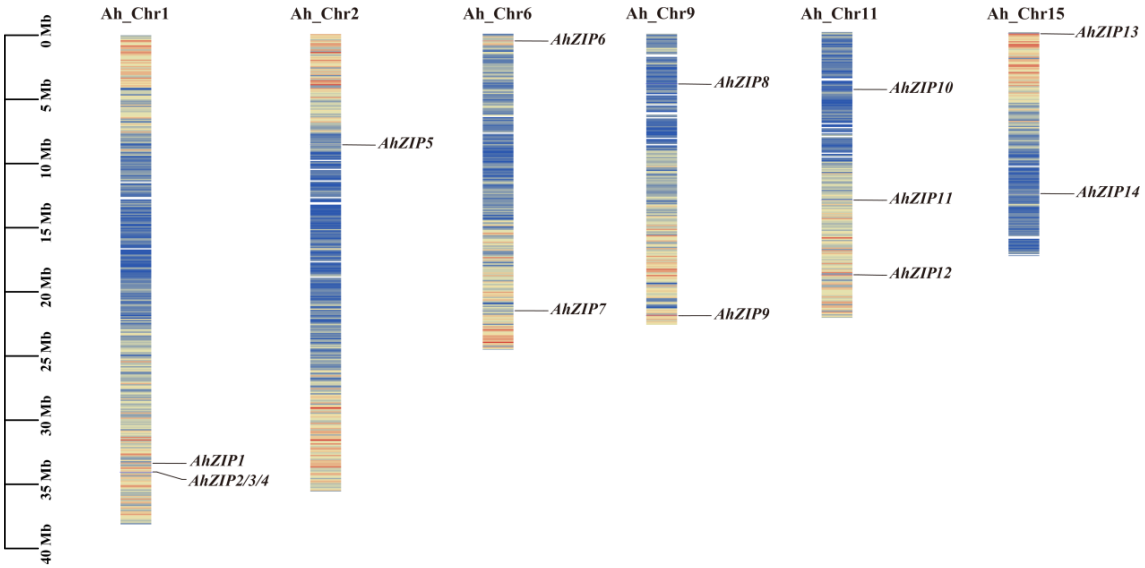

Fig. 1 Chromosomal distribution of *A. hypochondriacus ZIP* genes. The scale is in megabases (Mb). The chromosome number is indicated at the top of each chromosome.

https://doi.org/10.48130/grares-0026-0031

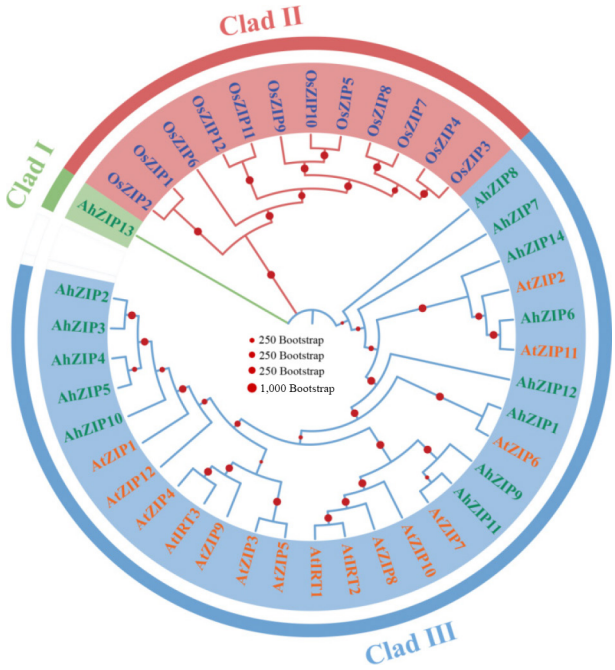

Fig. 2 Phylogenetic relationship of *A. hypochondriacus* (green) ZIP proteins with those of *A. thaliana* (orange) and *O. sativa* (blue). MEGA12 software was used to construct an unrooted phylogenetic tree based on alignments of ZIP proteins using the NJ method with 1,000 bootstrapped replicates.

proteins were concentrated in Clade II, AtZIP proteins were distributed only in Clade III, and AhZIP proteins were present in both Clade I and Clade III. These results indicate that there is a clear evolutionary divergence barrier between the ZIP proteins of monocotyledonous and dicotyledonous plants, and that AhZIP proteins are phylogenetically closely related to AtZIP proteins but distantly related to OsZIP proteins.

Gene structure and conserved motif compositions of *AhZIP* genes

For further insights into the functions of *AhZIP* genes, the exon–intron patterns of *AhZIP* genes were investigated by aligning the genome sequences with the CDS sequences of *AhZIP* genes. Another phylogenetic tree was generated using 14 AhZIP proteins, and it was suggested that genes having a closer evolutionary relationship normally revealed a more similar gene structure (Fig. 3a, b). For example, the homolog pairs *AhZIP1* and *AhZIP9* have similar gene structures with three exons and two introns. *AhZIP7* is most related to *AhZIP8*, and both of them share the most complex gene structures.

The conserved motif sites of AhZIP proteins were explored with the MEME online program, and 15 conserved motifs were characterized in these AhZIP proteins (Fig. 3c). The divergence of motif composition occurs among different clades, implying that AhZIP proteins in different clades may perform different functions in *A. hypochondriacus*. In general, AhZIP proteins with closer relationships within the same clade shared more similar motifs. In Clade III, AhZIP2, AhZIP3, AhZIP4, AhZIP5, and AhZIP10 were closely related in the phylogenetic tree and exhibited highly similar motif compositions, suggesting that they may play similar roles in *A. hypochondriacus*. Furthermore, the motif organizations of AhZIP7, AhZIP8, and AhZIP13 showed some differences, indicating functional divergence among the Clade III AhZIP proteins. Collectively, these results suggested that the exon–intron structures of the *AhZIP* genes and the motif organizations of the AhZIP proteins were consistent with the phylogenetic classification of AhZIPs in *A. hypochondriacus*.

The transmembrane domains of 14 AhZIP proteins were predicted using TMHMM 2.0 (Supplementary Fig. S1). The results showed that all AhZIP family members are transmembrane proteins, with 5–16 transmembrane domains regularly distributed in their sequences. Among them, AhZIP13 has the largest number of transmembrane regions, and AhZIP11 has the fewest. The transmembrane domains of most members are concentrated in the middle and posterior segments of the sequences, which provides a structural basis for their metal transport function.

Expression profiles of *AhZIP* genes in different tissues

To further determine the tissue expression pattern of *AhZIP* genes, public data of the expression profiles of *A. hypochondriacus* genes in different organs/tissues, including leaves, roots, floral, maturing seeds, immature seeds, dry tissue, stems, and green cotyledons were searched and analyzed for identifying the physiological functions of *AhZIP* genes (Fig. 4). As shown in Fig. 4, *AhZIP*

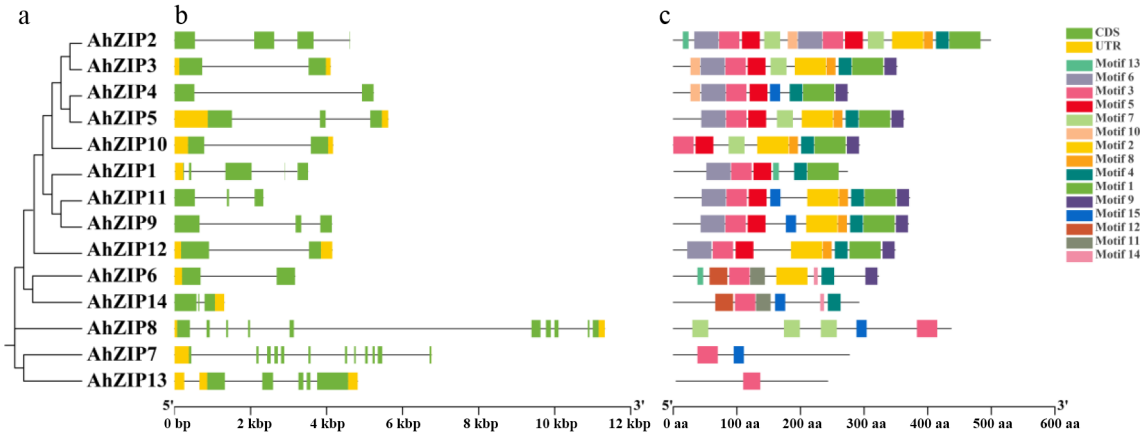

Fig. 3 Characterization of *A. hypochondriacus ZIP* genes and their encoding proteins. (a) Phylogenetic tree of AhZIP protein constructed using the NJ method. (b) The distribution of exons and introns in *AhZIP* genes. The green columns, black lines, and yellow columns represent exons, introns, and upstream/downstream regions. (c) Conserved motif compositions of AhZIP proteins. Motifs 1–15 were identified using MEME software, and each motif is shown with a specific color.

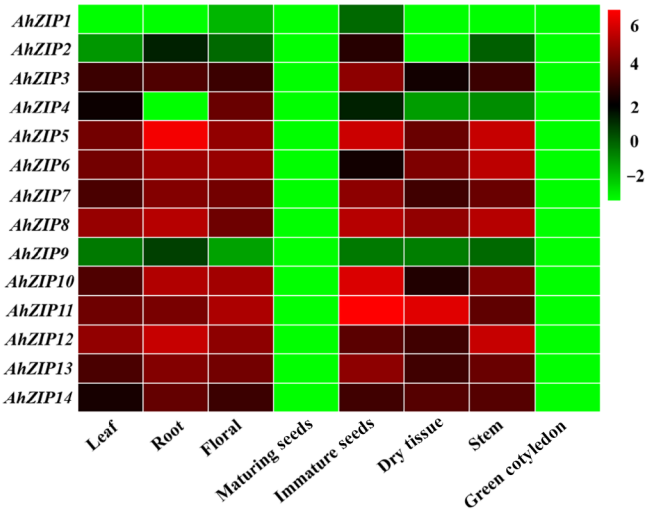

Fig. 4 Heatmap representation of the expression profiles of *A. hypochondriacus ZIP* genes in different tissues. Transcript levels of *AhZIP* genes were obtained from the public transcriptome database of *A. hypochondriacus* (NCBI BioProject: PRJNA290113). The transcript values were normalized to generate $\log_2$ expression values. Then $\log_2$-transformed values were subjected to R software (15.2) to analyze the expression patterns. The heatmap for the gene expression patterns was generated by the online program Omicshare (www.omicshare.com/tools/Home/Soft/heatmap).

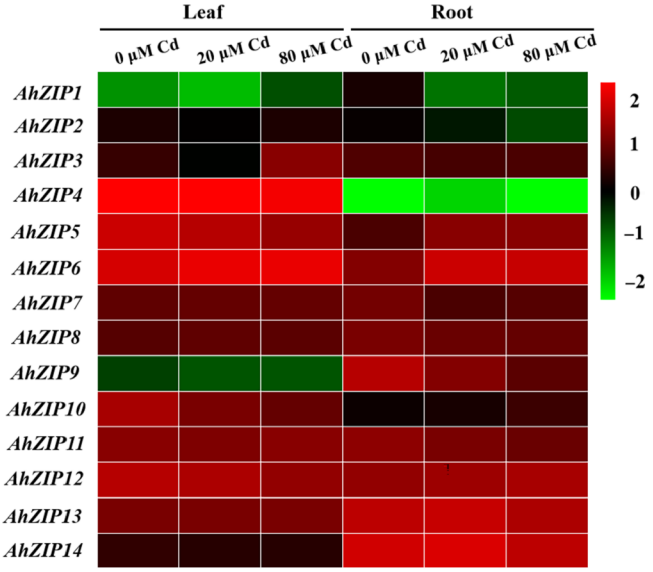

Fig. 5 Heatmap representation of the expression profiles of *A. hypochondriacus ZIP* genes under treatment with different concentrations of Cd. Transcript levels of *AhZIP* genes were determined by quantitative RT-PCR, using *AhActin* as a quantification control. Data were processed with Microsoft Excel 2021. The average of three biological replicates was used to generate $\log_2$ expression values. Then $\log_2$-transformed values were subjected to R software (15.2) to analyze the expression patterns. The heatmap for the gene expression patterns was generated by the online program Omicshare (www.omicshare.com/tools/Home/Soft/heatmap).

genes exhibited organ/tissue-specific expression, and they were barely expressed in the green cotyledons and maturing seeds. The root and stem systems were the sites for absorption and transportation of metal ions. Most of these genes were highly expressed in roots and stems except for *AhZIP1*, *AhZIP2*, *AhZIP4*, and *AhZIP9*. *AhZIP5/8/10/11/12* were accumulated extremely abundantly in root tissues, and *AhZIP5/6/8/11/12* had relatively high expression levels in stem tissues, indicating that these *AhZIP* genes may play crucial roles in the absorption and transportation of metal ions. Moreover, *AhZIP8/11/13* were also expressed highly in leaf tissues, suggesting that they may be related to leaf formation. *AhZIP5/10/11* had extremely high expression levels in immature seeds, implying their roles in seed development.

Expression levels of *AhZIP* genes were altered under Cd treatments at different concentrations

The expression levels of *AhZIP* genes after exposure to Cd were examined via Real-Time Quantitative Polymerase Chain Reaction (RT-qPCR) to investigate their potential roles in response to heavy metal stress (Fig. 5). The results showed that the expression of *AhZIP3* was strongly induced in leaf tissues after treatment with 80 μM Cd, whereas the expression of *AhZIP3* was unchanged in root tissues after Cd treatment. *AhZIP5* and *AhZIP6* exhibited clearly upregulated expression patterns in the presence of Cd stress in root tissues, but neither of them showed a response to Cd exposure in leaf tissues. These results revealed that *AhZIP3/5/6* had special roles in the absorption and transportation of Cd, respectively.

Expression levels of *AhZIP* genes in response to Cd treatments for different times

The expression profiles of *AhZIP* genes in response to Cd at different times were also studied. RT-qPCR analysis suggested that these *AhZIP* genes displayed varied expression profiles over time under Cd treatments. The expression of *AhZIP1/2/3/9/10/12/13/14* in root tissues was obviously induced under Cd treatment, but the expression of these genes peaked at different times. Moreover, the expression levels of *AhZIP4/5/6/7/8* in root tissues decreased under the Cd treatments (Fig. 6a). In leaf tissues, the expression of most *AhZIP* genes was inhibited except for *AhZIP3/5/6/9* under Cd stress (Fig. 6b). *AhZIP1/5/6/10/11/12/13/14* exhibited opposite expression patterns in root and leaf tissues, and the rest of the *AhZIP* genes showed similar expression trends in root and leaf tissues.

Subcellular localization of AhZIPs

To further investigate the roles of AhZIP proteins in the absorption and accumulation of Cd, *AhZIP3/5/6* were identified as the candidate genes and supposed to be involved in Cd resistance. The subcellular localizations of AhZIP3/5/6 proteins were analyzed. Vectors expressing *AhZIP3/5/6* fused with the *eGFP* marker gene and driven by the cauliflower mosaic virus (CaMV) 35S promoter were constructed. The AhZIP3/5/6 proteins were transiently expressed in foliar epidermis cells of tobacco (*Nicotiana benthamiana*). As shown in Fig. 7, using the endoplasmic reticulum (ER) marker, clear signals of co-localization of the fusion proteins and marker around the ER area were visualized, suggesting that AhZIP proteins were localized to the ER.

Function validation of *AhZIP* genes in yeast

AhZIP3/5/6 were heterologously expressed respectively in the Cd-sensitive mutant yeast strain *ycf1* to test whether AhZIP3/5/6 confers tolerance to and accumulation of Cd. As shown in Fig. 8a, there was no difference in growth state between the yeast cells carrying the empty vector and those expressing AhZIP proteins when the yeast cells were dripped onto the medium with 0 μM and 30 μM $CdCl_2$. The growth inhibition of AhZIP transformants was

https://doi.org/10.48130/grares-0026-0031

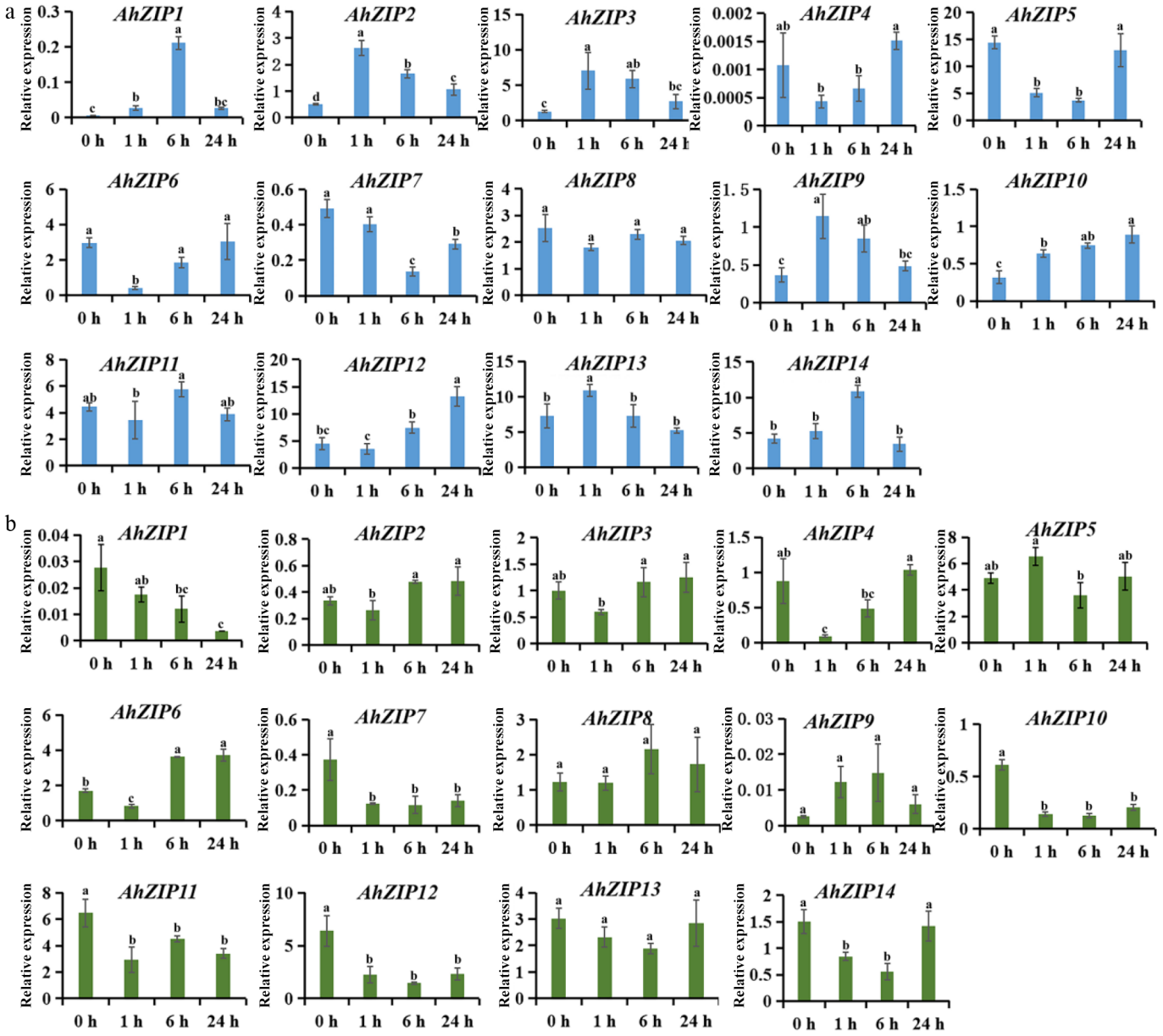

Fig. 6 Expression patterns of the *A. hypochondriacus ZIP* genes under Cd treatments for different times. (a) Expression of *AhZIP* genes in response to Cd^{2+} stress in root tissues; (b) expression of *AhZIP* genes response to Cd^{2+} stress in leaf tissues. Transcript levels of *AhZIP* genes were determined by quantitative RT-PCR, using *AhActin* as a quantification control. Mean values and standard deviations are shown from three independent experiments. For each gene, statistical significance among time points (0, 1, 6, and 24 h) was determined by one-way ANOVA followed by Tukey's HSD *post hoc* test. Different lowercase letters above the bars indicate significant differences ($p < 0.05$); bars sharing the same letter are not significantly different.

more severe than that of the empty vector when the yeast cells were dripped onto the media with 60 μM and 100 μM $CdCl_2$. Yeast's growth in a liquid SD-Ura medium containing 60 μM $CdCl_2$ was analyzed over time, and the growth curve assay revealed that *ycf1*_EV grew better than ycf1_*AhZIP3/5/6*, illustrating that Cd exerted a more profound inhibition effect on ycf1_*AhZIP3/5/6* than ycf1_EV (Fig. 8b). To further assess whether the growth inhibition resulted from high accumulation of Cd, the intracellular Cd content of these yeast transformants was determined. The accumulation of Cd in ycf1_AhZIP3/5/6 was significantly higher than in ycf1_EV (Fig. 8d). The results revealed that the expression of *AhZIP3/5/6* genes may facilitate the import of Cd inside the yeasts. These results suggest that the expression of *AhZIP3* may promote the absorption of Cd by plants.

Discussion

The zinc–iron transporter ZIP family in plants plays a key role in the absorption, transport, and homeostatic regulation of Cd^{2+}. Cd^{2+} mainly enters plant cells through the transport channels of ZIP proteins for divalent metal ions such as Zn^{2+} and Fe^{2+}[42]. In *A. thaliana*, AtIRT1 can mediate the active absorption of Cd by the roots under Cd stress[43]. OsZIP5 and OsZIP9 can jointly enhance absorption of Cd by the roots in rice[30]. *OsIRT1* and *OsIRT2* are upregulated under iron deficiency conditions and synergistically mediate the absorption of Cd^{2+}[44,45]. OsZIP2 can mediate the influx of Cd into the xylem parenchyma cells of roots, indirectly regulating the absorption and transport of Cd by the roots[33]. In addition, during the transport of Cd^{2+}, ZIP proteins are responsible for loading the Cd^{2+} absorbed by the roots into the xylem and transporting

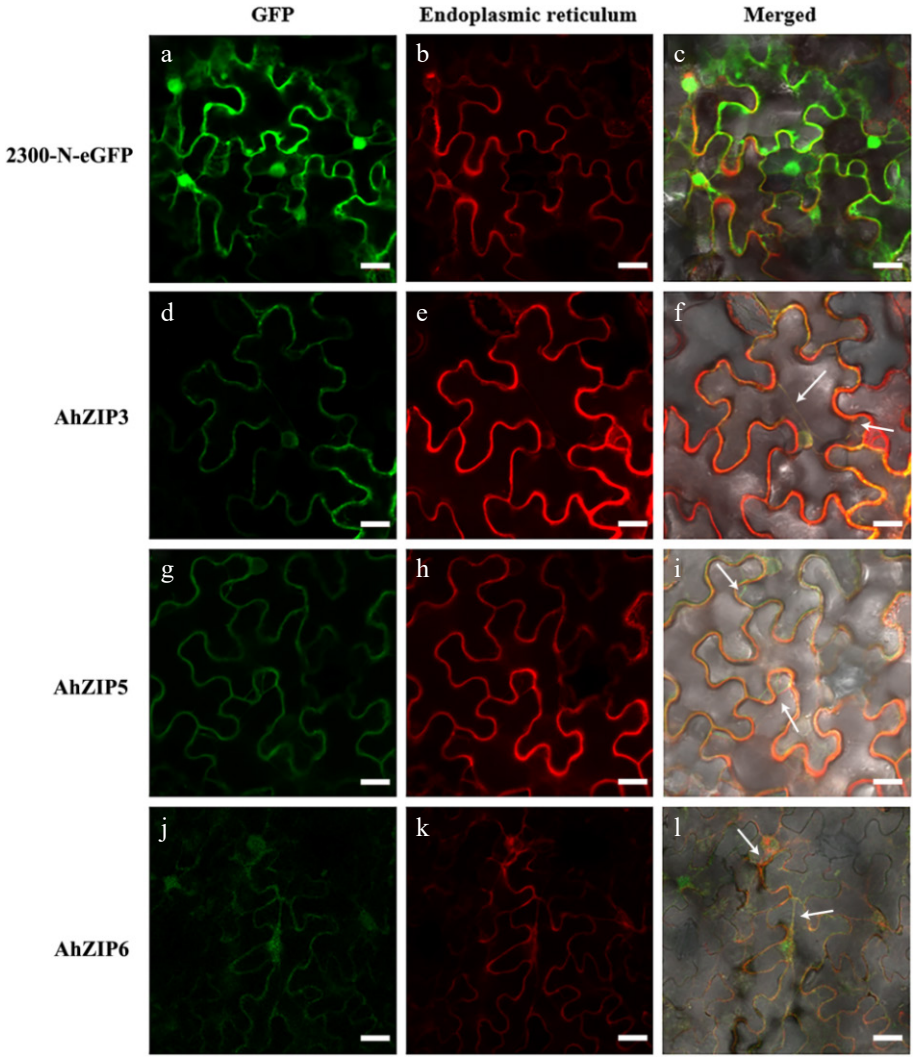

Fig. 7 Subcellular localization of AhZIP-GFP fusion proteins. (a)–(c) Confocal images of 2300-N-eGFP proteins. (a) 2300-N-eGFP; (b) ER-marker RFP-KDEL; (c) merged images of (a) and (b). (d)–(f) Confocal images of AhZIP3 proteins. (d) AhZIP3-GFP; (e) ER-marker RFP-KDEL; (f) merged images of (d) and (e). (g)–(i) Confocal images of AhZIP5 proteins. (g) AhZIP5-GFP; (h) ER-marker RFP-KDEL; (i) merged images of (g) and (h). (j)–(l) Confocal images of AhZIP6 proteins. (j) AhZIP6-GFP; (k) ER-marker RFP-KDEL; (l) merged images of (j) and (k). ER, endoplasmic reticulum; RFP, red fluorescent protein, eGFP, enhanced green fluorescent protein; KDEL, abbreviation of the four-amino-acid (Lys-Asp-Glu-Leu) residue sequence. Bars = 20 μm.

them to the aboveground parts. SmZIP8 of *Salix matsudana* Koidz. can significantly promote the transport of Cd^{2+} from the roots to aboveground parts and increase Cd accumulation in the aboveground parts[46]. ZIP proteins also play a key role in the cross-tissue transport of Cd^{2+} in plants. OsZIP7 can participate in the intervascular transport of Cd at nodes of *O. sativa*, promoting the distribution and transport of Cd[29]. Similarly, TaZIP7 in wheat (*Triticum aestivum*) is involved in the redistribution of Cd from nodes to grains, and its downregulation increases Cd retention in the nodes and reduces Cd accumulation in the grains[47]. In present study, 14 *AhZIP* genes were identified. *AhZIP* genes showed obvious tissue-specific expression, and their expression levels in the roots and leaves were significantly affected by Cd stress (Figs. 4–6). In roots, the expression levels of *AhZIP1/2/3/9/10/12/13/14* were significantly induced by Cd (Fig. 6a), indicating that these genes may be mainly involved in the absorption and transport of Cd by the roots. In leaves, the expression of *AhZIP3* was specifically induced, suggesting that it may be involved in the transport, distribution, or detoxification of Cd in aboveground parts (Fig. 6b). These findings indicate that *AhZIP* genes may play an important role in the absorption and enrichment of Cd^{2+}.

ZIP proteins are mainly localized in plasma membrane, ER, or vacuolar membrane, reflecting the specificity of their functions. Plasma membrane-localized ZIP proteins can directly mediate the transmembrane absorption of rhizosphere Cd^{2+} and the loading of intracellular Cd^{2+} into the xylem. For example, OsIRT1/OsZIP5 in *O. sativa*[42], and SmZIP8 in *S. matsudana*[46] all regulate the absorption and long-distance transport of Cd through their plasma membrane localization. ER-localized proteins can sequester Cd^{2+} through ER compartmentalization, significantly reducing cytoplasmic Cd toxicity and achieving intracellular Cd enrichment[48]. In soybean (*Glycine max*), the ER-localized GmHMA3 sequesters Cd into the ER of roots, thereby limiting its translocation to the stems[49]. In rice, OsZIP1, which is localized to both the ER and the plasma membrane, acts as a metal efflux transporter that limits excess Cd accumulation[25]. AtHMA3 in *A. thaliana*, which is localized to the vacuolar membrane, mediates the transport of Cd^{2+} into the vacuole for long-term storage, thereby achieving efficient intracellular Cd enrichment and reducing its toxicity[50]. Furthermore, some ZIP proteins exhibit multilocalization across organelles. For example, OsZIP1 in rice is localized to both the ER and the plasma membrane, and functions

https://doi.org/10.48130/grares-0026-0031

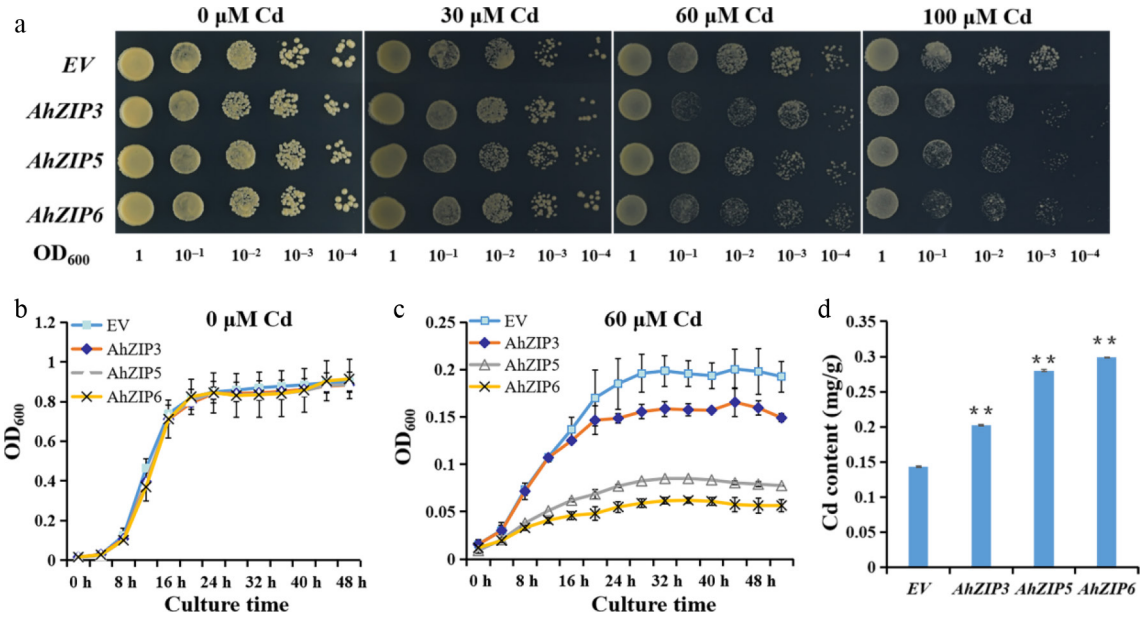

Fig. 8 Functional validation of *AhZIP* genes in yeast. (a) Drop assay of the *ycf1* transformants on media with different concentrations of $CdCl_2$. (b) Growth assay of the *ycf1* transformants incubated in the normal medium; (c) growth assay of the *ycf1* transformants incubated in a medium with 60 μM $CdCl_2$. (d) Total Cd contents in *ycf1* transformants after 48 h of incubation supplemented with 60 μM $CdCl_2$. EV, *ycf1* strains expressing the empty vector; AhZIP3/5/6, *ycf1* strains expressing *AhZIP* genes. For comparisons between two groups, Student's *t*-test (two-tailed, unpaired) was used, and significance levels are indicated as * $p < 0.05$, ** $p < 0.01$, and *** $p < 0.001$.

as a metal efflux transporter that limits excess Zn, Cu, and Cd accumulation in plants[25]. Our study showed that AhZIP3/5/6 proteins are localized to the ER (Fig. 7), and their heterologous overexpression can increase the enrichment of Cd^{2+} in yeast (Fig. 8), indicating that they may sequester Cd^{2+} through ER compartmentalization, transport free Cd^{2+} in the cytoplasm to the ER lumen for storage, reduce cytoplasmic Cd toxicity, and achieve preliminary intracellular Cd^{2+} enrichment.

Yeast, a unicellular fungus, possesses only simple vacuoles and lacks plant-type vacuolar structures. Moreover, the Cd-sensitive *ycf1* mutant strain used in this study is defective in the YCF1-mediated vacuolar compartmentalization of Cd, a key detoxification pathway in yeasts[51], and its tolerance threshold for Cd is far lower than that of plants with tissue and organ specialization, such that even a small amount of excess Cd can markedly disturb its metabolism[52]. Under Cd treatment, heterologous expression of *AhZIP* genes in yeast promotes the accumulation of Cd^{2+} within the cells, raising the concentration of free Cd^{2+} in the cytoplasm and thereby inhibiting the yeast's growth (Fig. 8). As a more advanced organism and a Cd hyperaccumulator, *A. hypochondriacus* may have developed complex Cd storage locations and detoxification systems. AhZIP proteins may realize efficient Cd enrichment while avoiding cytoplasmic toxicity through ER compartmentalization in *A. hypochondriacus*. The phenotypic analysis in yeast confirms the function of AhZIP proteins in the absorption and enrichment of Cd. The ER localization also suggests the detoxification function of AhZIP proteins in *A. hypochondriacus*. Heterologous expression in yeast is a well-established and efficient system for the functional validation of plants' metal transporter genes, owing to the clear genetic background of yeast, the simplicity of its genetic manipulation, and the availability of well-characterized metal homeostasis mutants such as the Cd-hypersensitive *ycf1* strain used in this study, which together provide a sensitive platform for detecting the Cd transport activity of AhZIP proteins. However, as a unicellular organism, yeast lacks the tissue differentiation, intercellular transport, and organ-level homeostatic regulation of plants; moreover, the subcellular localization and regulatory context of heterologous proteins in yeast may differ from those in planta. Therefore, the yeast phenotypes observed here provide direct evidence for the Cd transport capacity of AhZIP3/5/6 but should be interpreted cautiously, and the definitive physiological functions of AhZIP proteins require further validation in plants.

Conclusions

Fourteen *AhZIP* genes were systematically identified at the whole-genome level in *A. hypochondriacus*. These genes exhibited distinct tissue-specific expression patterns and responded to Cd stress. Subcellular localization assays revealed that the AhZIP3, AhZIP5, and AhZIP6 proteins are localized to the ER. Heterologous expression in yeast confirmed that these genes positively regulate the uptake and accumulation of Cd. Collectively, AhZIP proteins may play critical roles in the uptake, transport, and detoxification of Cd in *A. hypochondriacus*. These findings provide important gene resources and a theoretical foundation for further elucidating the molecular mechanisms underlying Cd hyperaccumulation.

Author contributions

The authors confirm their contributions to the paper as follows: study conception and design: Lu R, Cao X, Xu Q; data collection: Cao X, Pan M, Wu H, Yu W; analysis and interpretation of results: Cao X, Yu W, Luo X, Wang C, Liu N; draft manuscript preparation: Lu R, Hu L, Cao X. All authors reviewed the results and approved the final version of the manuscript.

Data availability

The data that support the findings of this study are available upon request from the author. The *A. hypochondriacus* genome sequences and gene annotation data used in this study were obtained from

the Phytozome database (https://phytozome-next.jgi.doe.gov; *A. hypochondriacus* v2.1). The transcriptome data used for the tissue-specific expression analysis were retrieved from the NCBI Sequence Read Archive under BioProject accession PRJNA290113 (www.ncbi.nlm.nih.gov/bioproject/290113).

Acknowledgments

This work was supported by Yuelushan Laboratory Talent Program (Grant No. 2024RC2064), the Science Foundation for the Excellent Youth of the Hunan Provincial Education Department (Grant No. 24B0189), the Science & Technology Specific Projects in Agricultural High-tech Industrial Demonstration Area of the Yellow River Delta (2022SZX13), and the Postgraduate Scientific Research Innovation Project of Hunan Province (Grant No. CX20251088).

Conflict of interest

The authors declare that they have no competing interests.

Supplementary information accompanies this paper online at: https://doi.org/10.48130/grares-0026-0031.

Dates

Received 7 August 2026; Revised 25 September 2026; Accepted 9 October 2026; Published online 4 November 2026

References

[1] Hou D, Jia X, Wang L, McGrath SP, Zhu YG, et al. 2025. Global soil pollution by toxic metals threatens agriculture and human health. *Science* 388:316–321

[2] Guan M, Xia Y, Zhang W, Chen M, Cao Z. 2025. A review of reducing cadmium pollution in the rice–soil system in China. *Foods* 14:1747

[3] Yu Y, Alseekh S, Zhu Z, Zhou K, Fernie AR. 2024. Multiomics and biotechnologies for understanding and influencing cadmium accumulation and stress response in plants. *Plant Biotechnology Journal* 22:2641–2659

[4] Antoniadis V, Levizou E, Shaheen SM, Ok YS, Sebastian A, et al. 2017. Trace elements in the soil-plant interface: phytoavailability, translocation, and phytoremediation–a review. *Earth-Science Reviews* 171:621–645

[5] Ashraf S, Ali Q, Zahir ZA, Ashraf S, Asghar HN. 2019. Phytoremediation: environmentally sustainable way for reclamation of heavy metal polluted soils. *Ecotoxicology and Environmental Safety* 174:714–727

[6] Qin G, Niu Z, Yu J, Li Z, Ma J, et al. 2021. Soil heavy metal pollution and food safety in China: effects, sources and removing technology. *Chemosphere* 267:129205

[7] Cao X, Dong Q, Mao L, Yang X, Wang X, et al. 2025. Enhanced phytoextraction technologies for the sustainable remediation of cadmium-contaminated soil based on hyperaccumulators—a review. *Plants* 14:115

[8] Lei L, Cui X, Li C, Dong M, Huang R, et al. 2022. The cadmium decontamination and disposal of the harvested cadmium accumulator *Amaranthus hypochondriacus* L. *Chemosphere* 286:131684

[9] Yu G, Liu J, Long Y, Chen Z, Sunahara GI, et al. 2020. Phytoextraction of cadmium-contaminated soils: comparison of plant species and low molecular weight organic acids. *International Journal of Phytoremediation* 22:383–391

[10] Yang L, Kang Y, Liu J, Li N, Sun H, et al. 2022. Foliar spray with rutin improves cadmium remediation efficiency excellently by enhancing antioxidation and phytochelatin detoxification of *Amaranthus hypochondriacus*. *International Journal of Phytoremediation* 24:1060–1070

[11] Sterckeman T, Thomine S. 2020. Mechanisms of cadmium accumulation in plants. *Critical Reviews in Plant Sciences* 39:322–359

[12] Wu X, Chen J, Yue X, Wei X, Zou J, et al. 2019. The zinc-regulated protein (ZIP) family genes and glutathione s-transferase (GST) family genes play roles in Cd resistance and accumulation of pak choi (*Brassica campestris* ssp. *chinensis*). *Ecotoxicology and Environmental Safety* 183:109571

[13] Clemens S, Aarts MGM, Thomine S, Verbruggen N. 2013. Plant science: the key to preventing slow cadmium poisoning. *Trends in Plant Science* 18:92–99

[14] Palusińska M, Barabasz A, Kozak K, Papierniak A, Maślińska K, et al. 2020. Zn/Cd status-dependent accumulation of Zn and Cd in root parts in tobacco is accompanied by specific expression of *ZIP* genes. *BMC Plant Biology* 20:37

[15] Yue X, Song J, Fang B, Wang L, Zou J, et al. 2021. BcNRAMP1 promotes the absorption of cadmium and manganese in *Arabidopsis*. *Chemosphere* 283:131113

[16] Robe K, Lefebvre-Legendre L, Cleard F, Barberon M. 2025. Four ZIPs contribute to Zn, Fe, Cu and Mn acquisition at the outer root domain. *PLoS Genetics* 21:e1011796

[17] Eide D, Broderius M, Fett J, Guerinot ML. 1996. A novel iron-regulated metal transporter from plants identified by functional expression in yeast. *Proceedings of the National Academy of Sciences of the United States of America* 93:5624–5628

[18] Rogers EE, Eide DJ, Guerinot ML. 2000. Altered selectivity in an *Arabidopsis* metal transporter. *Proceedings of the National Academy of Sciences of the United States of America* 97:12356–12360

[19] Krausko M, Labajová M, Peterková D, Jásik J. 2021. Specific expression of *AtIRT1* in phloem companion cells suggests its role in iron translocation in aboveground plant organs. *Plant Signaling & Behavior* 16:1925020

[20] Vert G, Barberon M, Zelazny E, Séguéla M, Briat JF, et al. 2009. *Arabidopsis* IRT2 cooperates with the high-affinity iron uptake system to maintain iron homeostasis in root epidermal cells. *Planta* 229:1171–1179

[21] Lin YF, Liang HM, Yang SY, Boch A, Clemens S, et al. 2009. *Arabidopsis* IRT3 is a zinc-regulated and plasma membrane localized zinc/iron transporter. *New Phytologist* 182:392–404

[22] Milner MJ, Seamon J, Craft E, Kochian LV. 2013. Transport properties of members of the ZIP family in plants and their role in Zn and Mn homeostasis. *Journal of Experimental Botany* 64:369–381

[23] Ochoa Tufiño V, Almira Casellas M, van Duynhoven A, Flis P, Salt DE, et al. 2025. *Arabidopsis thaliana* Zn transporter genes *ZIP3* and *ZIP5* provide the main Zn uptake route and act redundantly to face Zn deficiency. *The Plant Journal* 121:e17251

[24] Lee S, An G. 2009. Over-expression of *OsIRT1* leads to increased iron and zinc accumulations in rice. *Plant, Cell & Environment* 32:408–416

[25] Liu XS, Feng SJ, Zhang BQ, Wang MQ, Cao HW, et al. 2019. OsZIP1 functions as a metal efflux transporter limiting excess zinc, copper and cadmium accumulation in rice. *BMC Plant Biology* 19:283

[26] Ishimaru Y, Masuda H, Suzuki M, Bashir K, Takahashi M, et al. 2007. Overexpression of the OsZIP4 zinc transporter confers disarrangement of zinc distribution in rice plants. *Journal of Experimental Botany* 58:2909–2915

[27] Lee S, Jeong HJ, Kim SA, Lee J, Guerinot ML, et al. 2010. OsZIP5 is a plasma membrane zinc transporter in rice. *Plant Molecular Biology* 73:507–517

[28] Lee S, Kim SA, Lee J, Guerinot ML, An G. 2010. Zinc deficiency-inducible *OsZIP8* encodes a plasma membrane-localized zinc transporter in rice. *Molecules and Cells* 29:551–558

[29] Tan L, Zhu Y, Fan T, Peng C, Wang J, et al. 2019. *OsZIP7* functions in xylem loading in roots and inter-vascular transfer in nodes to deliver Zn/Cd to grain in rice. *Biochemical and Biophysical Research Communications* 512:112–118

[30] Tan L, Qu M, Zhu Y, Peng C, Wang J, et al. 2020. ZINC TRANSPORTER5 and ZINC TRANSPORTER9 function synergistically in zinc/cadmium uptake. *Plant Physiology* 183:1235–1249

https://doi.org/10.48130/grares-0026-0031

[31] Zhang X, Kong J, Yu L, Wang A, Yang Y, et al. 2024. Functional characterization of *Fagopyrum tataricum ZIP* gene family as a metal ion transporter. *Frontiers in Plant Science* 15:1373066

[32] Yu R, Li D, Du X, Xia S, Liu C, et al. 2017. Comparative transcriptome analysis reveals key cadmium transport-related genes in roots of two pak choi (*Brassica rapa* L. ssp. *chinensis*) cultivars. *BMC Genomics* 18:587

[33] Li MZ, Hu DW, Liu XQ, Zhang R, Liu H, et al. 2024. The OsZIP2 transporter is involved in root-to-shoot translocation and intervascular transfer of cadmium in rice. *Plant, Cell & Environment* 47:3865−3881

[34] Li Y, Zhang D, Wen H, Peng J, Wu J, et al. 2025. BjZIP1, a plasma membrane-localized transporter, mediates cadmium and zinc uptake in *Brassica juncea*. *Plant Cell Reports* 44:275

[35] Gong F, Qi T, Hu Y, Jin Y, Liu J, et al. 2022. Genome-wide investigation and functional verification of the ZIP family transporters in wild emmer wheat. *International Journal of Molecular Sciences* 23:2866

[36] Maślińska-Gromadka K, Barabasz A, Palusińska M, Kozak K, Antosiewicz DM. 2021. Suppression of *NtZIP4A/B* changes Zn and Cd root-to-shoot translocation in a Zn/Cd status-dependent manner. *International Journal of Molecular Sciences* 22:5355

[37] Zhang Z, Chen N, Zhang Z, Shi G. 2022. Genome-wide identification and expression profile reveal potential roles of peanut *ZIP* family genes in zinc/iron-deficiency tolerance. *Plants* 11:786

[38] Lightfoot DJ, Jarvis DE, Ramaraj T, Lee R, Jellen EN, et al. 2017. Single-molecule sequencing and Hi-C-based proximity-guided assembly of amaranth (*Amaranthus hypochondriacus*) chromosomes provide insights into genome evolution. *BMC Biology* 15:74

[39] Potter SC, Luciani A, Eddy SR, Park Y, Lopez R, et al. 2018. HMMER web server: 2018 update. *Nucleic Acids Research* 46:W200−W204

[40] Kumar S, Stecher G, Suleski M, Sanderford M, Sharma S, et al. 2024. MEGA12: molecular evolutionary genetic analysis version 12 for adaptive and green computing. *Molecular Biology and Evolution* 41:msae263

[41] Vera Hernández FP, Martínez Núñez M, Ruiz Rivas M, Vázquez Portillo RE, Bibbins Martínez MD, et al. 2018. Reference genes for RT-qPCR normalisation in different tissues, developmental stages and stress conditions of amaranth. *Plant Biology* 20:713−721

[42] Yang Y, Chen S, Liu H, Chen H, Lu Z, et al. 2025. Plant ZIP transporter: functional analysis on metal uptake, transport, and homeostasis. *Plant Physiology and Biochemistry* 229:110336

[43] Vert G, Grotz N, Dédaldéchamp F, Gaymard F, Guerinot ML, et al. 2002. IRT1, an *Arabidopsis* transporter essential for iron uptake from the soil and for plant growth. *The Plant Cell* 14:1223−1233

[44] Nakanishi H, Ogawa I, Ishimaru Y, Mori S, Nishizawa NK. 2006. Iron deficiency enhances cadmium uptake and translocation mediated by the Fe^{2+} transporters OsIRT1 and OsIRT2 in rice. *Soil Science and Plant Nutrition* 52:464−469

[45] Tao J, Lu L. 2022. Advances in genes-encoding transporters for cadmium uptake, translocation, and accumulation in plants. *Toxics* 10:411

[46] Zou J, Han J, Wang Y, Jiang Y, Han B, et al. 2022. Cytological and physiological tolerance of transgenic tobacco to Cd stress is enhanced by the ectopic expression of *SmZIP8*. *Plant Science* 319:111252

[47] Xiao C, Yang H, Chen X, Li J, Cai X, et al. 2024. Application of lanthanum at the heading stage effectively suppresses cadmium accumulation in wheat grains by downregulating the expression of *TaZIP7* to increase cadmium retention in nodes. *Plants* 13:2921

[48] De Caroli M, Furini A, DalCorso G, Rojas M, Di Sansebastiano GP. 2020. Endomembrane reorganization induced by heavy metals. *Plants* 9:482

[49] Wang Y, Wang C, Liu Y, Yu K, Zhou Y. 2018. GmHMA3 sequesters Cd to the root endoplasmic reticulum to limit translocation to the stems in soybean. *Plant Science* 270:23−29

[50] Morel M, Crouzet J, Gravot A, Auroy P, Leonhardt N, et al. 2009. AtHMA3, a P_{1B}-ATPase allowing Cd/Zn/Co/Pb vacuolar storage in *Arabidopsis*. *Plant Physiology* 149:894−904

[51] Li ZS, Lu YP, Zhen RG, Szczypka M, Thiele DJ, et al. 1997. A new pathway for vacuolar cadmium sequestration in *Saccharomyces cerevisiae*: YCF1-catalyzed transport of bis(glutathionato)cadmium. *Proceedings of the National Academy of Sciences of the United States of America* 94:42−47

[52] Wysocki R, Tamás MJ. 2010. How *Saccharomyces cerevisiae* copes with toxic metals and metalloids. *FEMS Microbiology Reviews* 34:925−951

Copyright: © 2026 by the author(s). Published by Maximum Academic Press, Fayetteville, GA. This article is an open access article distributed under Creative Commons Attribution License (CC BY 4.0), visit https://creativecommons.org/licenses/by/4.0/.